*Astronomy & Astrophysics* manuscript no. GRB111117A
Thursday 1st June, 2017


# The host galaxy of the short GRB 111117A at $z = 2.211^{\star}$

J. Selsing[1], T. Krühler[2], D. Malesani[1,3], P. D'Avanzo[4], J. Palmerio[5], S. D. Vergani[6], J. Japelj[7], B. Milvang-Jensen[1], D. Watson[1], P. Jakobsson[8], Z. Cano[9], V. D'Elia[10], A. de Ugarte Postigo[9,1], J. P. U. Fynbo[1], A. Gomboc[11], K. E. Heintz[8,1], A. J. Levan[12], M. Sparre[1,13], N. R. Tanvir[14], and C. C. Thöne[9]

[1] Dark Cosmology Centre, Niels Bohr Institute, University of Copenhagen, Juliane Maries Vej 30, 2100 København Ø, Denmark
[2] Max-Planck-Institut für extraterrestrische Physik, Giessenbachstraße, 85748 Garching, Germany
[3] DTU Space, National Space Institute, Technical University of Denmark, Elektrovej 327, DK-2800 Lyngby, Denmark
[4] INAF - Osservatorio Astronomico di Brera, via E. Bianchi 46, I-23807, Merate (LC), Italy
[5] Sorbonne Universités, UPMC Univ. Paris 6 et CNRS, UMR 7095, Institut d'Astrophysique de Paris, 98 bis bd Arago, 75014 Paris, France
[6] GEPI, Observatoire de Paris, PSL Research University, CNRS, Univ. Paris Diderot, Sorbonne Paris Cité, 5 Place Jules Janssen, 92195 Meudon, France
[7] Anton Pannekoek Institute for Astronomy, University of Amsterdam, Science Park 904, 1098 XH Amsterdam, The Netherlands
[8] Centre for Astrophysics and Cosmology, Science Institute, University of Iceland, Dunhagi 5, 107 Reykjavík, Iceland
[9] Instituto de Astrofísica de Andalucía (IAA-CSIC), Glorieta de la Astronomía s/n, E-18008, Granada, Spain.
[10] INAF-Osservatorio Astronomico di Roma, Via Frascati 33, I-00040 Monteporzio Catone, Italy; ASI-Science Data Centre, Via del Politecnico snc, I-00133 Rome, Italy
[11] University of Nova Gorica, Vipavska 13, 5000 Nova Gorica, Slovenia.
[12] Department of Physics, University of Warwick, Coventry CV4 7AL, UK
[13] Heidelberger Institut für Theoretische Studien, Schloss-Wolfsbrunnenweg 35, 69118 Heidelberg, Germany
[14] Department of Physics and Astronomy, University of Leicester, University Road, Leicester, LE1 7RH, UK

Received/ accepted

**ABSTRACT**

It is notoriously difficult to localize short $\gamma$-ray bursts (sGRBs) and their hosts to measure their redshifts. These measurements, however, are critical to constrain sGRB progenitors and delay time models. Here, we present spectroscopy of the host galaxy of GRB 111117A and measure its redshift to be $z = 2.211$. This makes GRB 111117A the most distant high-confidence short GRB detected to date. Our spectroscopic redshift supersedes a lower redshift value for this burst previously estimated from photometry.
We use the spectroscopic redshift, as well as new imaging data to constrain the nature of the host galaxy as well as physical parameters of the GRB. The rest frame X-ray derived hydrogen column density, for example, is high compared to a complete sample of sGRBs and seems to follow the evolution with redshift as traced by the hosts of long GRBs (lGRBs). This is consistent with the proportion of the sGRB population originating in late-type galaxies live in similar environments to that of lGRB hosts.
The host lies in the brighter end of the expected host brightness distribution at $z = 2.211$, and is actively forming stars. Using the host as a benchmark for redshift determination, we find that less than 55 per cent of all sGRB redshifts should be missed due to host faintness at $z \sim 2$. The high redshift of GRB 111117A is evidence against a lognormal delay-time model for sGRBs through the predicted redshift distribution of sGRBs, which is very sensitive to high-$z$ sGRBs.
From the age of the universe at explosion time, an initial progenitor separation of $a_0 < 3.2\ R_{\odot}$ is required in the case of a binary neutron star system. This puts constraints on the progenitor system evolution up to the time of explosion.

**Key words.** Gamma-ray burst: individual: GRB 111117A —

## 1. Introduction

There is now mounting evidence that most short-duration gamma-ray bursts (GRBs) come from the merger of neutron stars (NSs), either with another NS, or a black hole, due to their apparent association with kilonovae (Barnes & Kasen 2013, Tanvir et al. 2013, Yang et al. 2015, Jin et al. 2016, Rosswog et al. 2016). The absence of associated supernovae in deep searches (e.g. Hjorth et al. 2005b, Fox et al. 2005, Hjorth et al. 2005a) supports this idea and distinguishes the physical origin of sGRBs from their long-duration counterparts.

The host galaxies of short GRBs are diverse. They are more massive and less actively star-forming on average than long GRB hosts (Fong et al. 2013), while in some cases, no host galaxy can be identified (Berger 2010, Tunnicliffe et al. 2014). Together with their position within their hosts (Fong & Berger 2013), this suggests a progenitor system that can be very long-lived, and is associated with stellar mass rather than star-formation rate (Berger 2014). The median redshift for sGRBs is $z \sim 0.5$ (Berger 2014), and because most of these measurements come from the associated hosts, it is arguably biased towards lower redshifts.

The total lifetimes of NS binaries depends on their initial separations and subsequent inspiral times, and impacts the timing and distribution of the enrichment of the ISM and subsequent stars and planets with heavy $r$-process elements (van de Voort et al. 2014, Wallner et al. 2015, Ji et al. 2016). Some limits can be calculated based on models of star-formation histories of, and the spatial distribution of sGRBs in, their host galaxies (Berger

$^{\star}$ Based on observations collected at the European Southern Observatory, Paranal, Chile, Program ID: 088.A-0051 and 091.D-0904.

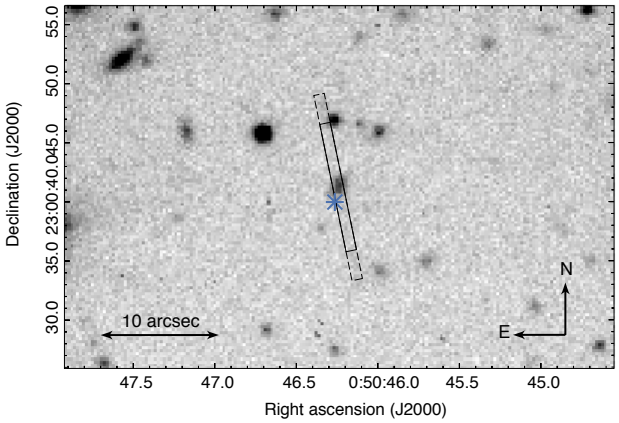


**Fig. 1.** Imaging of the field of GRB 111117A with the X-shooter slit overlaid. Only one slit is shown, despite four epochs of spectroscopic observations because of the similarity in position angle. The image is the FORS2 *R*-band image andthe blue asterisk indicates the GRB position as derived from the *Chandra* observations in Sakamoto et al. (2013). The errorcircle of the *Chandra*-position is too small to be visible in the image.

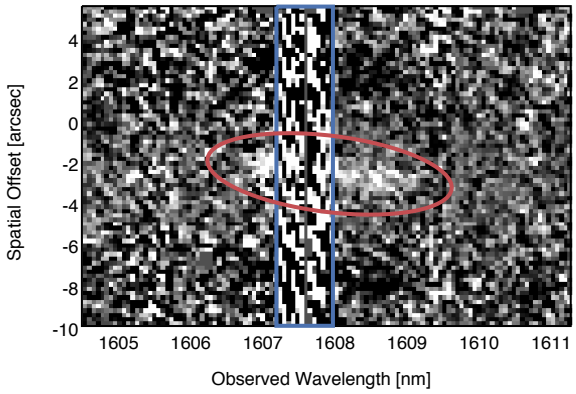


**Fig. 2.** 2D-image of the [O III]$\lambda$5007 emission line. The location of a bright skyline is marked by the blue box. The location of the emission line is indicated with the red ellipse. Because the host is observed in nodding-mode, negative images of the emission line appear on both sides in the spatial direction.

2014). The most distant cosmological bursts, however, offer direct, hard limits.

In this *Letter* we present the spectrum of the host galaxy of the short GRB 111117A ($T_{90}$ = 0.46 s) and measure its redshift to be $z$ = 2.211. This value is significantly higher than the previously estimated redshift based on photometric studies. We present the GRB's rest frame properties based on this new distance compared to previous analyses (Margutti et al. 2012, Sakamoto et al. 2013) and revisit the host properties derived from the new solution to the SED fit.

Throughout this *Letter* we use the $\Lambda$CDM cosmology provided by Planck Collaboration et al. (2016) in which the universe is flat with $H_0$ = 67.7 km s$^{-1}$ and $\Omega_m$ = 0.307 and report all magnitudes in the AB system.

## 2. Observations and results

### 2.1. Spectroscopic observations and analysis

Spectroscopic observations were carried out using the cross-dispersed echelle spectrograph, VLT/X-shooter (Vernet et al. 2011), at four seperate epochs. The burst was followed up 38 hours after the Burst Alert Telescope (BAT) trigger under ESO programme 088.A-0051 (PI: Fynbo) and again later using a different ESO program 091.D-0904 (PI: Hjorth). X-shooter can cover the wavelength range from 3000 Å to 24 800 Å (21 000 Å when the *K*-band blocking filter is used) across three spectroscopic arms, simultaneously illuminated through the use of dichroics. The bias-correction, flat-fielding, order tracing, wavelength calibration, rectification, and flux calibration is then carried out using the VLT/X-shooter pipeline version 2.8.4 (Modigliani et al. 2010). The observations are combined and extracted using scripts described in Selsing et al. 2017 (in prep.) and available online[1]. The signal-to-noise of the continuum in the near-infrared arm is too low to use the optimal extraction algorithm (Horne 1986) and therefore the extraction is carried out with a simple aperture.

[1] https://github.com/jselsing/XSGRB_reduction_scripts

An overview of the spectroscopic observations is given in Table 1, and the position of the slit on the target is shown in Fig. 1.

We determine a redshift of $z$ = 2.211 from the simultaneous detection of emission lines interpreted as Ly$\alpha$, [O II], H$\beta$, [O III]$\lambda$5007, and H$\alpha$, with H$\beta$ detected at low significance ($\sim 3\sigma$). H$\alpha$ is only visible in the first epoch, due to the *K*-band blocking filter used for the remainder observations. The nebular lines exhibit a spatial extent of $\sim 1\farcs5$ and show significant velocity structure along the slit. A drop in the continuum to the blue of the Ly$\alpha$ line further supports the inferred redshift.

Using the luminosity of H$\alpha$, we can infer the star-formation rate (SFR) of a galaxy (Kennicutt 1998). At the redshift of the GRB host, H$\alpha$ is observed at 21 000 Å where the night sky is very bright. In addition, several bright sky-lines intersect the line, making an accurate estimate of the H$\alpha$-flux difficult. We obtain a limit on the SFR by integrating the part of H$\alpha$ free of contamination and correcting for the missing flux using the line shape. After converting the Kennicutt (1998) relation to a Chabrier (2003) initial mass function using Madau & Dickinson (2014), we derive a limit of $SFR > 7 M_\odot$ yr$^{-1}$. From the SED-fit (Sect. 2.2), and the detection of Ly$\alpha$, the host is constrained to contain very little or no dust, which is why we do not apply a dust-correction to the measured H$\alpha$ flux here.

### 2.2. Imaging observations and SED analysis

In addition to the spectroscopy presented above, we imaged the field of GRB 111117A in multiple broad-band filters using the VLT equipped with FORS2 (*gRIz* filters) and HAWK-I ($JHK_s$ filters), long after the burst has faded. These new data are complemented by a re-analysis of some of the imagery used in Margutti et al. (2012) and Sakamoto et al. (2013) that are available to us here (GTC *gri*-band, TNG *R*-band, and Gemini *z*-band). A log of the photometric observations and measured brightnesses is given in Table 2.

All data were reduced, analyzed and fitted in a similar manner as described in detail in Krühler et al. (2011) and, more recently, in Schulze et al. (2016). Very briefly, we use our own `python` and IRAF routines to perform a standard reduction which includes bias/flat-field correction, de-fringing (if necessary), sky-subtraction, and stacking of individual images. The photometry of the host was tied against magnitudes of field stars

from the SDSS and 2MASS catalogs in the case of $grizJHK_s$ filters. For the $R$ and $I$-band photometry we used the color transformations of Lupton[2]. We convert all magnitudes into the AB system if necessary, and correct for the Galactic foreground of $E_{B-V} = 0.027$ mag.

The multi-color spectral energy distribution (SED) is fit by Bruzual & Charlot (2003) single stellar population models based on a Chabrier (2003) initial mass function in *LePhare* (Ilbert et al. 2006), where the redshift is fixed to the spectroscopic value of $z = 2.211$. The best model is obtained with an unreddened galaxy template, and returns physical parameters of absolute magnitude ($M_B = -22.0 \pm 0.1$ mag), stellar mass ($\log(M_\star/M_\odot) = 9.9 \pm 0.2$), stellar population age ($\tau = 0.5^{+0.5}_{-0.3}$ Gyr) and star-formation rate ($SFR_{\rm SED} = 11^{+9}_{-4} M_\odot\,{\rm yr}^{-1}$).

Noteworthy is the discrepancy of our new VLT/FORS2 photometry and the re-analysis of Gemini data to the $z$-band measurements of Margutti et al. (2012) and Sakamoto et al. (2013). Both of these authors report $z$-band photometry that is brighter by 0.8 mag to 1.0 mag than our value, whereas data taken in bluer filters are in excellent agreement. In fact, the large $i - z$ color is mistakenly interpreted as a 4000 Å break driving the galaxy photometric redshift of the earlier works. Using the revised photometry from Table 2, the photometric redshift of the galaxy is $z_{\rm phot} = 2.04^{+0.19}_{-0.21}$, consistent with the spectroscopic value at the 1 $\sigma$ confidence level.

### 2.3. X-ray temporal and spectral analysis

We retrieved the automated data products provided by the *Swift*-XRT GRB repository[3] (Evans et al. 2009). The X-ray afterglow light curve can be fit with a single power-law decay with index $\alpha = 1.27^{+0.12}_{-0.10}$. We performed a time-integrated spectral analysis using data in photon counting (PC) mode in the widest time epoch where the $0.3 - 1.5$ keV to $1.5 - 10$ keV hardness ratio is constant (namely, from $t - T_0 = 205$ s to $t - T_0 = 203.5$ ks, for a total of 29.1 ks of data) to prevent spectral changes that can affect the X-ray column density determination. The obtained spectrum is well described by an absorbed power-law model. The best-fit spectral parameters are a photon index of $2.1 \pm 0.4$ and an intrinsic hydrogen column density $N_{\rm H}$ of $2.4^{+2.4}_{-1.6} \times 10^{22}$ cm$^{-2}$ ($z = 2.211$), assuming a Galactic $N_{\rm H}$ in the burst direction of $4.1 \times 10^{20}$ cm$^{-2}$ Willingale et al. (2013).

## 3. Reinterpretation of restframe properties

### 3.1. Classification

As already pointed out (Margutti et al. 2012, Sakamoto et al. 2013), GRB 111117A securely belongs the short class of GRBs. Because the observed classification indicators, $T_{90}$ and hardness ratio, do not depend strongly on redshift (Littlejohns et al. 2013), the updated redshift does not change this designation significantly. The intrinsic luminosity increases, as visible in the X-ray light curve in Fig. 3, but it still is sub-luminous compared to the majority of long GRBs. Bromberg et al. (2013) investigated the degree to which the long and short population distributions overlap and quantified the certainty in the class membership. GRB 111117A has $96^{+3}_{-5}$ percent probability of being short. Compared to the other two sGRB candidates at high redshift, GRB060121 (de Ugarte Postigo et al. 2006, Levan et al. 2006) at $1.7 \lesssim z \lesssim 4.5$ ($17^{+14}_{-15}$ per cent) and GRB090426 (Antonelli et al. 2009, Levesque et al. 2010, Thöne et al. 2011) at $z = 2.609$ ($10^{+15}_{-10}$ per cent), the certainty in class membership for GRB 111117A is much higher.

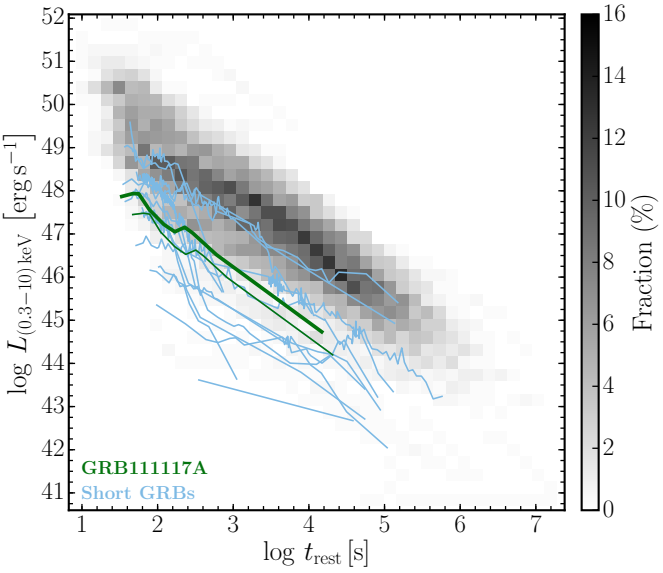


**Fig. 3.** Restframe XRT lightcurve of GRB 111117A, compared to the general population of XRT lightcurves of GRBs. The grey shared region is a compilation of long GRB lightcurves where the color represents density and the light blue is other short GRB lightcurves for which redshifts has been determined. Despite the remarkably high redshift, the luminosity is comparable to the bulk of the short burst population and still subluminous compared to the lGRB population.

### 3.2. Restframe $N_{\rm H}$

We plot the recalculated $N_{\rm H}$ in Fig. 4 where we compare with the distributions of complete samples of both long and short GRBs. The lGRB sample is from Arcodia et al. (2016) and the sGRB sample is from D'Avanzo et al. (2014). 17 of the 99 long bursts do not have redshifts and likewise 5 out of 16 for the short sample. Bursts without redshifts have been excluded for both groups. GRB 111117A occupies a unique position in Fig. 4 with the highest $N_H$ of all short burst. The short sample, excluding GRB 111117A, is located at low redshifts ($z < 1$) and is found to populate a similar column density environment to long GRBs at similar redshifts (D'Avanzo et al. 2014). The inferred hydrogen column for GRB 111117A seems to follow the trend with increasing $N_H$ as a function of redshift as found for the long GRB afterglows (Arcodia et al. 2016).

### 3.3. Host galaxy

As the majority of short GRBs (Fong et al. 2013), the host of GRB 111117A is a late-type galaxy and is entirely consistent in terms of stellar mass and stellar age with the general population of short GRB hosts ($\langle M_* \rangle = 10^{10.1} M_\odot$ and $\langle \tau_* \rangle = 0.3$ Gyr) (Leibler & Berger 2010). Being a late-type host, both the stellar mass and sSFR are entirely within the range expected for the hosts of sGRBs (Behroozi et al. 2014). The SFR is ~1 order

[2] https://www.sdss3.org/dr8/algorithms/sdssUBVRITransform.php
[3] http://www.swift.ac.uk/xrt_products/00507901

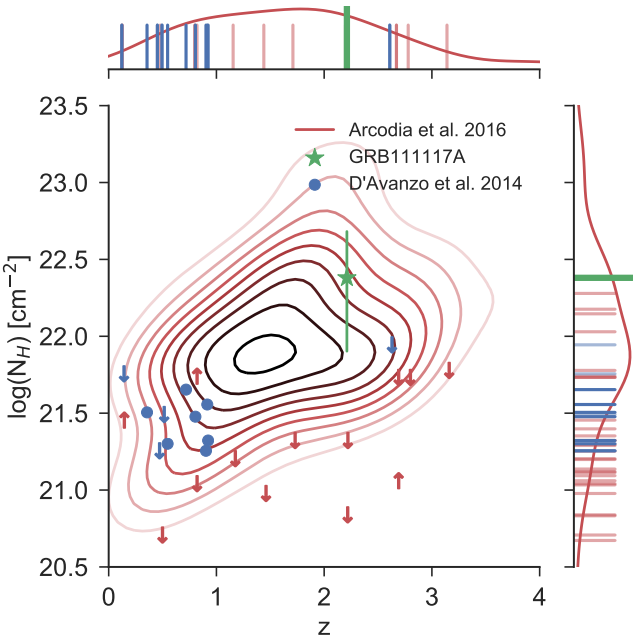


**Fig. 4.** Rest frame, X-ray derived hydrogen column densities for GRB 111117A compared to complete samples of both long and short populations. In red we show the sample of lGRBs from Arcodia et al. (2016). The detections are replaced with contours for clarity and the limits are shown with arrows. In blue is the sample of sGRBs from D'Avanzo et al. (2014). GRB 111117A is an outlier from the short sample, but seems to follow the distribution of long GRBs.

of magnitude higher than the typical SFR for short GRB hosts galaxies (Berger 2014) and more similar to the SFRs found in the hosts of long GRBs at a corresponding redshift (Krühler et al. 2015). The high SFR is partly a selection effect, because a less star-forming galaxy would exhibit weaker emission lines, thus making the redshift harder to determine. Additionally, it is natural to expect some evolution in the hosts of sGRBs with redshift as illustrated in Sect. 3.2.

## 4. Implications for redshift distribution of short GRBs

A single sGRB at high redshift does little in terms of constraining the redshift distribution and therethrough the progenitor channels. In particular, other short-GRB hosts could be missed because they are intrinsically fainter and thus this high-$z$ event is only detected due to the brightness of the host. Berger (2014) compiled a sample of sGRB host luminosities, normalized by the characteristic galaxy luminosity at their respective redshift, $L_B/L_B^\star$. 26 out of 39 hosts (66 per cent) in the sample have redshifts. To convert the SED-inferred $M_B$ of GRB 111117A to $L_B/L_B^\star$, we use the characteristic absolute B-band magnitude of the Schechter function for the blue galaxies ($U-V<0.25$) in the redshift window $2.0 \leq z \leq 2.5$ from Marchesini et al. (2007) and find $L_B/L_B^\star = 1.2$, which is brighter than 70 per cent of the hosts in Berger (2014) with measured $L_B/L_B^\star$.

If we assume that we are able to obtain emission-line redshifts from hosts with $R < 25$ mag (Krühler et al. 2012), then we would have missed around 30 per cent (8 out of 26 from the sample of Berger 2014 with measured $L_B/L_B^\star$), if they were at the redshift of GRB 111117A. Because the average SFR of galaxies hosting lGRBs is higher than for galaxies hosting sGRBs, the fraction of missed burst redshifts is likely higher although the cosmic SFR evolution could play a role in improving redshift determinability.

A fraction of the bursts missing redshift are host-less and is therefore likely at moderate redshifts (Tunnicliffe et al. 2014), but should some of the remainder be at high redshift, the missed fraction will increase. If we assume that *all* the bursts that are missing redshifts in Berger (2014) are at high-$z$ and missed due to host faintness, 22 out of 39 hosts (55 per cent) would be missed at $z = 2.211$. This serves as an upper limit on the fraction of missed burst at high-$z$ and illustrates that we are likely *not* missing a large fraction of sGRBs redshift at $z \approx 2$, due to host faintness.

The theoretical redshift distribution of sGRBs depends on the type of delay-time function used to model the progenitor system. The redshift of GRB 111117A puts constraints on the type of delay-time models suitable for modeling. The likelihood preferred lognormal time delay models investigated in Wanderman & Piran (2015) predicts a rate of sGRBs at $z = 2.211$, $\sim$ two orders of magnitude lower compared to peak rate ($z = 0.9$). It is stated in Wanderman & Piran (2015) that this preference depends critically on the absence of non-collapsar sGRB at $z \gtrsim 1.2$. The redshift of the burst, on the other hand, is close to the expected peak in sGRB rate calculated for the power law models (Behroozi et al. 2014, Wanderman & Piran 2015).

## 5. Constraints on the progenitor separation

At $z = 2.211$, the age of the universe is 3 Gyr. If the progenitor systems of sGRBs are the merger of two neutron stars, this sets a hard upper limit to the coalescence timescale for such a system. In the absence of other mechanisms, the timescale of the orbital decay of the system is set by the energy loss due to gravitational waves, which in turn is set by the mass of constituent compact objects and the separation of the two (Postnov & Yungelson 2014). If we assume that the formation timescale of the first galaxies is short compared to the time since the big bang (Richard et al. 2011) and if we assume a mass of 1.4 $M_\odot$ for each of the neutron stars at the time of system formation, this places a hard upper limit on the initial separation, $a_0$, of the two neutron stars of $a_0 < 3.2\ R_\odot$.

If we use the stellar population age from our SED fit, then we obtain a (softer) limit on the initial separation of $a_0 < 2.1\ R_\odot$. However, this does not account for the possibility there could be an underlying stellar population of older stars from a previous star-formation epoch. The delay time between formation and explosion is well accommodated by the models of Belczynski et al. (2006), although the longest formation channels are excluded. This is especially true given the late type nature of the host (O'Shaughnessy et al. 2008).

## 6. Conclusions

In this *Letter*, we have provided a revised, spectroscopic redshift for the short GRB 111117A based on emission lines setting it at $z = 2.211$. This value supersedes and corrects the previous photometric redshift of Margutti et al. (2012) and Sakamoto et al. (2013). The erroneous redshift estimate of previous authors is attributed to a discrepancy in the measured $z$-band magnitude.

The rest-frame parameters of the burst and the conditions of the burst environment have been recalculated using the new distance. The X-ray derived hydrogen column density towards GRB 111117A is the highest within a complete sample of short

hosts, but is indicative of an evolution with redshift as found for the hosts of long GRBs.

The SFR of the host is in the upper end of the sGRB host SFR distribution and this helped us to measure the redshift for this galaxy. Despite the moderate age and high $N_{\rm H}$, almost no dust is present.

Although a single burst carries little leverage in terms of constraining the redshift distribution of sGRB, the high redshift of GRB 111117A needs to be accommodated in progenitor models. A lognormal delay time model predicts a very low volumetric density of bursts at $z = 2.211$, whereas a power law delay time model peaks near GRB 111117A. If more sGRBs are at similarly high redshifts, but are missed due to the faintness of their hosts, a lognormal delay time model will be disfavored. Compared to a sample of short GRB hosts, GRB 111117A is more luminous than 70 per cent of the sample with measured luminosities. Conservatively, for 55 per cent of the sGRB hosts, we would be unable to determine a redshift should they be at a similar redshift as GRB 111117A. This implies that we are *not* missing a large fraction of the sGRBs at $z \sim 2$.

Using the age of the universe at the time of explosion allows us to set constraints on the maximal separation between the engine constituents at the time of formation. We find that the maximal separation for two neutron stars at formation time is $a_0 < 3.2\ R_\odot$, which excludes some of the formation channels with the longest timescales.

All data, code and calculation related to the paper along with the paper itself are available at `https://github.com/jselsing/GRB111117A`.

*Acknowledgements.* TK acknowledges support through the Sofja Kovalevskaja Award to P. Schady. CT acknowledges support from a Spanish National Research Grant of Excellence under project AYA 2014-58381-P and funding associated to a Ramón y Cajál fellowship under grant number RyC-2012-09984.

## References

Antonelli L. A., et al., 2009, A&A, 507, L45
Arcodia R., Campana S., Salvaterra R., 2016, A&A, 590, A82
Barnes J., Kasen D., 2013, ApJ, 775, 18
Behroozi P. S., Ramirez-Ruiz E., Fryer C. L., 2014, ApJ, 792, 123
Belczynski K., Perna R., Bulik T., Kalogera V., Ivanova N., Lamb D. Q., 2006, ApJ, 648, 1110
Berger E., 2010, ApJ, 722, 1946
Berger E., 2014, ARA&A, 52, 43
Bromberg O., Nakar E., Piran T., Sari R., 2013, ApJ, 764, 179
Bruzual G., Charlot S., 2003, MNRAS, 344, 1000
Chabrier G., 2003, PASP, 115, 763
D'Avanzo P., et al., 2014, MNRAS, 442, 2342
Evans P. A., et al., 2009, MNRAS, 397, 1177
Fong W., Berger E., 2013, ApJ, 776, 18
Fong W., et al., 2013, ApJ, 769, 56
Fox D. B., et al., 2005, Nature, 437, 845
Hjorth J., et al., 2005a, Nature, 437, 859
Hjorth J., et al., 2005b, ApJ, 630, L117
Horne K., 1986, PASP, 98, 609
Ilbert O., et al., 2006, A&A, 457, 841
Ji A. P., Frebel A., Chiti A., Simon J. D., 2016, Nature, 531, 610
Jin Z.-P., et al., 2016, Nat. Commun., 7, 12898
Kennicutt R. C., 1998, ARA&A, 36, 189
Krühler T., et al., 2011, A&A, 526, A153
Krühler T., et al., 2012, ApJ, 758, 46
Krühler T., et al., 2015, A&A, 581, A125
Leibler C. N., Berger E., 2010, ApJ, 725, 1202
Levan A. J., et al., 2006, ApJ, 648, L9
Levesque E. M., et al., 2010, MNRAS, 401, 963
Littlejohns O. M., Tanvir N. R., Willingale R., Evans P. A., O'Brien P. T., Levan A. J., 2013, MNRAS, 436, 3640
Madau P., Dickinson M., 2014, ARA&A, 52, 415
Marchesini D., et al., 2007, ApJ, 656, 42
Margutti R., et al., 2012, ApJ, 756, 63
Modigliani A., et al., 2010, SPIE Astron. Telesc. + Instrum., 7737, 773728
O'Shaughnessy R., Belczynski K., Kalogera V., 2008, ApJ, 675, 566
Planck Collaboration et al., 2016, A&A, 594, A13
Postnov K. A., Yungelson L. R., 2014, LRR, 17
Richard J., Kneib J.-P., Ebeling H., Stark D. P., Egami E., Fiedler A. K., 2011, Mon. Not. R. Astron. Soc. Lett., 414, L31
Rosswog S., Feindt U., Korobkin O., Wu M. R., Sollerman J., Goobar A., Martinez-Pinedo G., 2016, eprint arXiv:1611.09822
Sakamoto T., et al., 2013, ApJ, 766, 41
Schulze S., et al., 2016
Tanvir N. R., Levan A. J., Fruchter A. S., Hjorth J., Hounsell R. A., Wiersema K., Tunnicliffe R. L., 2013, Nature, 500, 547
Thöne C. C., et al., 2011, MNRAS, 414, 479
Tunnicliffe R. L., et al., 2014, MNRAS, 437, 1495
Vernet J., et al., 2011, A&A, 536, A105
Wallner A., et al., 2015, Nat. Commun., 6, 5956
Wanderman D., Piran T., 2015, MNRAS, 448, 3026
Willingale R., Starling R. L. C., Beardmore A. P., Tanvir N. R., O'Brien P. T., 2013, MNRAS, 431, 394
Yang B., et al., 2015, Nat. Commun., 6, 7323
de Ugarte Postigo A., et al., 2006, ApJ, 648, L83
van de Voort F., Quataert E., Hopkins P. F., Kere D., Faucher-Giguere C.-A., 2014, MNRAS, 447, 140

**Table 1.** Overview of the spectroscopic observations. JH in the slit width refers to observations where a K-band blocking filter has been used. The seeing is determined from the width of the spectral trace of a telluric standard star, taken close in time to the host observation. The spectral resolution, R, is measured from unresolved telluric absorption lines in the spectrum of the telluric standard star.

| Obs. Date | Exposure time (s) | | | Slit width | Airmass | Seeing | R |
|---|---|---|---|---|---|---|---|
| | UVB | VIS | NIR | (arcsec) | | (arcsec) | VIS/NIR |
| 2011-11-19T01:33 | $2 \times 2400$ | $2 \times 2400$ | $8 \times 600$ | 1.0/1.0/0.9 | 1.49 | 0.75 | 11600/6700 |
| 2013-07-15T09:02 | $2 \times 1200$ | $2 \times 1200$ | $8 \times 300$ | 1.0/1.0/0.9JH | 1.53 | 0.98 | 9600/8900 |
| 2013-08-03T07:37 | $2 \times 1200$ | $2 \times 1200$ | $8 \times 300$ | 1.0/1.0/0.9JH | 1.55 | 0.85 | 11400/11300 |
| 2013-08-03T08:34 | $2 \times 1200$ | $2 \times 1200$ | $8 \times 300$ | 1.0/1.0/0.9JH | 1.49 | 0.85 | 11400/11300 |

**Table 2.** Overview of the photometric observations.

| Obs. Date | Exptime | Telescope/Instrument | Filter | Airmass | Image Quality | Host Brightness[a] |
|---|---|---|---|---|---|---|
| | ks | | | | (arcsec) | ($\mathrm{mag_{AB}}$) |
| 2013-08-30T07:43 | 1.45 | VLT/FORS2 | $g$ | 1.55 | 0.99 | $24.08 \pm 0.09$ |
| 2011-11-17T20:07 | 0.80 | GTC/OSIRIS | $g$ | 1.15 | 1.67 | $24.13 \pm 0.09$ |
| 2011-11-17T20:07 | 1.20 | GTC/OSIRIS | $r$ | 1.11 | 1.50 | $23.93 \pm 0.08$ |
| 2013-07-17T08:37 | 1.45 | VLT/FORS2 | $R$ | 1.56 | 0.74 | $23.95 \pm 0.06$ |
| 2011-11-28T21:10 | 3.60 | TNG/LRS | $R$ | 1.01 | 1.08 | $23.96 \pm 0.13$ |
| 2011-11-17T20:07 | 0.36 | GTC/OSIRIS | $i$ | 1.08 | 1.50 | $23.89 \pm 0.23$ |
| 2013-08-03T09:23 | 1.35 | VLT/FORS2 | $I$ | 1.54 | 0.93 | $24.22 \pm 0.15$ |
| 2011-11-28T06:14 | 1.80 | Gemini/GMOS-N | $z$ | 1.01 | 0.84 | $24.24 \pm 0.47$ |
| 2013-07-13T09:33 | 1.08 | VLT/FORS2 | $z$ | 1.49 | 0.63 | $23.76 \pm 0.21$ |
| 2013-06-24T09:14 | 1.98 | VLT/HAWK-I | $J$ | 1.70 | 0.63 | $23.13 \pm 0.18$ |
| 2013-06-27T09:21 | 1.68 | VLT/HAWK-I | $H$ | 1.63 | 0.91 | $22.94 \pm 0.29$ |
| 2013-06-28T09:14 | 1.92 | VLT/HAWK-I | $K_s$ | 1.65 | 0.76 | $23.07 \pm 0.32$ |

**Notes.** [(a)] All magnitudes are given in the AB system and are not corrected for the expected Galactic foreground extinction corresponding to a reddening of $E_{B-V} = 0.027$ mag. **(Thomas, Can you help with the reference for the data which are not ours?)**